K-isomeric states in well-deformed heavy even-even nuclei

N. Minkov [*]
Institute of Nuclear Research and Nuclear Energy, Bulgarian Academy of Sciences, Tzarigrad Road 72, BG-1784 Sofia, Bulgaria

L. Bonneau [†] and P. Quentin
CENBG, UMR 5797, Université de Bordeaux, CNRS, F-33170 Gradignan, France

J. Bartel and H. Molique
IPHC, UMR 7178, Université de Strasbourg, CNRS, F-67000 Strasbourg, France

D. Ivanova
Military Medical Academy, Sofia, Bulgaria and University Hospital "Saint Ekaterina", Sofia, Bulgaria

(Received 7 November 2021; accepted 16 March 2022; published 28 April 2022)

We study excited states of two-quasiparticle (2qp) character in well-deformed even-even actinide and heavier nuclei exhibiting K isomerism within the framework of the Skyrme energy-density functional (SEDF) approach, including BCS pairing correlations with self-consistent blocking. We use the SIII SEDF parametrization with time-odd terms and seniority pairing residual interaction as in a previous study of magnetic moments in odd-mass nuclei [Phys. Rev. C **91**, 054307 (2015)]. The strength of the seniority interaction is determined through an overall fit on the 2_1^+ excitation energies along the lines of Phys. Rev. C **99**, 064306 (2019). Our calculations confirm the 2qp configurations reported in the literature providing an overall good agreement with the available data on isomeric energies. One notes, however, a few significant deviations such as in the $N = 142$ uranium and $N = 152$ nobelium isotopes, which are explained through known single-particle features of the SEDF used. Given the good predictive capability of the approach, we expect it to serve as a reliable tool in the search for similar kinds of qp excitations and to suggest additional or alternative qp configurations.

DOI: 10.1103/PhysRevC.105.044329

I. INTRODUCTION

Experimentally available even-even isotopes of actinide and heavier elements, further away from the magic numbers $N = 126$ and $Z = 82$, are known to possess an axially prolate rigid intrinsic deformation [1]. In these nuclei the existence of an isomeric activity whose excitation energy lies in the 1 MeV range is likely to correspond in most of the cases to a seniority-2 quasiparticle (qp) excitation. These quasiparticle states have a spin equal to K, the sum of the projections K_1 and K_2 of the single-particle (sp) angular momenta of each coupled sp state onto the intrinsic quantization axis. Such intrinsic configurations generate collective bands by coupling with the global rotation. Resulting from a sp type of excitation, they do not differ substantially in intrinsic shape with respect to the qp vacuum. Their isomeric character could thus be a consequence of the K value being significantly higher than what is allowed for a decay into states of collective bands built on the intrinsic ground state ($K = 0$ for the ground and β bands, $K = 2$ for γ bands, etc.). They are then called high-K isomers [2].

Large K values are likely to be obtained by a parallel coupling of sp states leading to $K = K_1 + K_2$ (with $K_1K_2 > 0$) with large enough values of $|K_1|$ and $|K_2|$. As is often noted (see for instance the review in Ref. [3]), the occurrence of states with high-K values in prolate deformed nuclei is mostly to be found in the second part of nuclear deformation regions (rare-earth or actinide and heavier elements) where many of the corresponding sp wave functions have fewer nodes in the z direction (chosen to be the symmetry axis). This explains why they are especially abundant, for instance, around $A = 180$, in the rare-earth region. Conversely, they are relatively scarce in actinides where this structural factor combined with an increasing (with A) instability reduces the possibility for their experimental observation [4], even though recent advances in spectroscopic studies of very heavy nuclei have been achieved.

Theoretically, one attempts to describe such states by approximating the many-body problem through the use of a one-body potential, e.g., of the Woods-Saxon type, or by applying a nonrelativistic or relativistic mean-field approach plus, in all cases, an appropriate albeit approximate treatment of pairing correlations. Obtaining in such a way low-energy qp excitations with spin $I = K$ and parity $\pi = \pi_1\pi_2$ (π_1 and π_2 being the parity of the coupled sp states) does not guarantee *a priori* their isomeric (metastable) character since, as

[*] nminkov@inrne.bas.bg
[†] bonneau@lp2ib.in2p3.fr

is well known, the latter depends on factors which are difficult to determine unambiguously in these approaches. The lifetime of a given state depends on its structural difference with another state to which it may decay as well as on the multipolarity and the matrix element of the electromagnetic transition connecting both states [3]. However, whereas the structural differences between the initial and the final state (such as coupling to collectivity, or K mixing as considered, e.g., in Ref. [5]) and their location in the spectrum favor the metastability of the former, it is not obvious whether the aforementioned simple theoretical descriptions are able to fully incorporate the underlying physical mechanism.

Nevertheless, one may hint at a global validity of the average potential in use whenever these theoretical approaches yield, in the right range of excitation energies, such 2qp structures with the correct quantum numbers. Furthermore, obtaining a good reproduction of the isomeric excitation energies E^* assesses the relevance of the relative sp energies of the two sp states under consideration. It is worth noting that such seniority-2 states provide a separate test for the spectra of each charge state, insofar as relevant data are available, in contrast to other quantities (e.g., moments of inertia) implying both neutrons and protons.

The study undertaken here is thus first meant as an evaluation of the single-particle spectral quality of the phenomenological effective Hamiltonian in use over the whole region of heavy deformed nuclei. It is obvious (see, e.g., Ref. [6]) that the study of such spectra in transfermium isotopes represents a further interest. Indeed, it may be used to estimate the possible extrapolation from existing data to study the contours of the so-called island of stability of superheavy elements. Here, our aim is purely methodological, namely to gain some degree of confidence that one may have vis-à-vis such a tentative assessment, as will be discussed in the conclusions.

However, the sp energy difference accounts only for a part of the isomeric energy. As pointed out long ago [7,8], the Pauli principle blocking effect, resulting in a decrease of the level density of sp states available for pair transfer, quenches significantly the pairing correlations in the isomeric states. As a consequence it generates a loss of binding energy in this state relative to the case in the ground state. For instance, calculations of Ref. [9] find that the isomeric energy of the 16^+ ^{178m_2}Hf state results from the additive contributions from the particle-hole excitation energy (1.5 MeV) and the pairing effects (1.1 MeV).

As compared to the wealth of theoretical studies addressing specifically the high-K isomeric states in rare-earth elements (see for instance the somewhat early review found in Sec. IV A of Ref. [10] following the pioneering work on noncollective high-spin states of the Lund-Warsaw Collaboration [11]), such studies for actinide and heavier elements are relatively less abundant. One should note the very early work of Soloviev and Siklos [12] using the Nilsson potential to compute E^* as the sum of relevant qp energies. Similar approaches have used the so-called universal parametrisation of the Woods-Saxon potential (see, e.g., Refs. [13–16]) or a two-center shell model approach [17]. Non-relativistic microscopic mean-field studies have also been carried out using a Skyrme force parametrization without [9] or with the inclusion of the time-reversal breaking effects [18] as well as similar calculations using the D1S parametrization of the Gogny force [19]. Finally, covariant density functional calculations have also been performed (see, e.g., [20]).

In this paper we extend the study initiated by the work reported in Ref. [18] where only two isotopes of uranium and two of plutonium were considered. Here, we attempt to make an exhaustive study of the seniority-2 K isomers in all relevant actinide and heavier isotopes selected according to some clear-cut criteria which will be explicitly given in Sect. III. This is achieved within a Hartree-Fock (HF) plus BCS framework, including some time-odd effects in the mean field [21] to describe the isomeric states within a self-consistent blocking approach. The well-studied (and rather well qualified for spectroscopic studies) Skyrme SIII parametrization [22] is chosen for the particle-hole channel. As will be seen below, this approach completely suffices not only to explore the systematic trends in the manifestation of K-isomeric excitations in the considered mass region but also to assess the relevance of their quasiparticle interpretation and the predictive capability of the applied Skyrme energy-density functional (SEDF) framework as a whole. A preliminary account of some of the results presented here was briefly discussed in Ref. [23].

The present paper is merely a first step towards a complete study of isomeric states which would include theoretical results on reduced electromagnetic probabilities pertaining to the deexcitation of such metastable states. It is our contention, however, that it is necessary to carefully study the effective Hamiltonian in use through its eigenenergies and static properties of its eigenstates before attempting to describe decay properties. To do so, we believe that the study of excitation energies of K isomers is a good method to judge of the quality of the mean-field potential, and this not only in terms of magic gaps, for instance, as often considered. The study of these gaps is indeed a valuable quality assessment but is merely of a (semiclassically) averaged nature à la Strutinsky, thus unable to discern correct level orderings within some relevant energy interval.

In Sec. II we sketch the theoretical approach and approximations in use together with some computational details. The selection of nuclei and isomeric states under study as well as the adjustment of the residual interaction are discussed in Secs. III and IV. The numerical results are presented and discussed in Sec. V. Section VI provides a summary and some concluding remarks, together with possible lines of improvement and/or extension of the present study.

II. THEORETICAL FRAMEWORK

Both the ground and excited states of the considered even-even nuclei are assumed to have axial symmetry in the intrinsic (body-fixed) frame. They are described within the Skyrme HF + BCS energy-density functional with self-consistent blocking (of two single-particle states) as explained in Ref. [21].

In particular, the time-reversal symmetry breaking at the one-body level in the excited nuclear states induces the removal of Kramers degeneracy in the single-particle energy

TABLE I. Harmonic-oscillator basis parameter b optimized for each considered nucleus. See text and Ref. [24] for its definition.

Nucleus	b (fm^{-1})
^{234}U	0.479
^{236}U	0.479
^{236}Pu	0.479
^{238}Pu	0.479
^{240}Pu	0.475
^{244}Pu	0.475
^{244}Cm	0.475
^{246}Cm	0.475
^{248}Cm	0.475
^{248}Cf	0.475
^{248}Fm	0.475
^{250}Fm	0.475
^{256}Fm	0.471
^{252}No	0.475
^{254}No	0.473
^{256}No	0.470
^{254}Rf	0.472
^{256}Rf	0.470

spectrum due to the self-consistent blocking. Moreover, because we use the SIII Skyrme parametrization, we work in the "minimal" scheme of Ref. [21] in which the only time-odd fields retained in the HF Hamiltonian are the spin and current vector fields.

The single-particle states are expanded in a truncated deformed harmonic-oscillator basis with axial symmetry. We use $N_0 + 1 = 17$ major oscillator shells together with basis parameters b and $\tilde{q}$ where b is the inverse of the oscillator length as displayed in Table I, and $\tilde{q}$ a dimensionless deformation parameter (ratio of oscillator frequencies along z and the perpendicular directions), consistently found in our calculations for the here considered nuclei to have a value of $\tilde{q} = 1.20$. These three parameters (N_0, b, and $\tilde{q}$) are defined in Ref. [24]. Finally we use for all quadratures 30 Gauss-Hermite mesh points in the z direction and 15 Gauss-Laguerre mesh points in the perpendicular direction.

The pairing contribution to the energy-density functional is calculated from the expectation value of a seniority residual interaction in a BCS state, supplemented by blocking when dealing with excited states. The parametrization of the nucleon-number dependence of the corresponding matrix elements is the same as in Ref. [21] and the fitting of its strength is presented in Sec. IV. The BCS equations are solved for all sp states with a smearing factor $f(e_i) = [1 + \exp\{(e_i - X - \lambda_q)/\mu\}]^{-1}$, where e_i is the energy of the sp state $|i\rangle$, X plays the role of a limiting factor with $X = 6$ MeV, λ_q is the chemical potential for the charge state q, and $\mu = 0.2$ MeV is a diffuseness parameter.

III. CHOICE OF THE SAMPLE OF NUCLEI

We have included in the present study 18 even-even isotopes of elements belonging to the actinide region and two nuclei beyond, namely ^{254,256}Rf. These have been chosen following two strong criteria or one weak criterion. The strong criteria are

(i) Well-deformed nuclei, yielding good rotor properties as assessed by the ratio $R_{4/2}$ of the energies of their 4_1^+ and 2_1^+ collective excited states being larger than 3.2. The basic set of data on these excitation energies is taken from the NNDC chart of nuclides [25], while additional information is taken from other sources, such as [26] for ^{250}Fm.

(ii) Nuclei with the presence of at least one K-isomeric state whose energy, spin, and parity are experimentally known or tentatively proposed. The basic set of data on this criterion is taken from the "Atlas of Nuclear Isomers" by Jain *et al.*, Ref. [27], while additional information is taken from later publications, such as Ref. [28] for ^{244}Pu.

The weaker criterion is

(iii) Nuclei with known excited states considered to be 2qp configurations not belonging to the K isomers documented as above, but whose excitation energies are in the same range. They have been retained to complete some isotopic or isotonic series of isomeric states. To this category we also assign nuclei with excitations for which the lifetimes are either not known or of the order of few nanoseconds, as well as nuclei entering most probably the overall deformation region but with no data allowing us to assess the $R_{4/2}$ ratio.

From the selected nuclei, thirteen isotopes satisfy the two strong criteria (i) and (ii). To them we have added five more nuclei qualifying under criterion (iii).

The first one is ^{238}Pu in which an isomeric activity has been found (with a half-life of 8.5 ns) for which a tentative 4^- assignment has been suggested [29]. It is specifically considered here in order to study the evolution with energy of a 5^- isomeric state based on the two-proton configuration ($K^\pi = 5/2^-, 5/2^+$) over a sequence of three plutonium isotopes from ^{236}Pu to ^{240}Pu.

Another one is ^{248}Cf whose 8^- state of 1.261 MeV [25] is interpreted in the literature as a neutron 2qp configuration [30]. Although, to the best of our knowledge, no experimental half-life is available for it, its inclusion in the study allows us to follow the evolution of the excitation energy of a 8^- isomeric state based on the two-neutron configuration ($K^\pi = 9/2^-, 7/2^+$) over a sequence of several $N = 150$ isotopes from ^{244}Pu to ^{252}No.

To this category we also assign ^{248}Fm for which a 6^+ state with a half-life of 10.1 ms is included in the K-isomer collection of Ref. [31], but we could not find any more detailed experimental information about it.

Finally, two more nuclei were also added under criterion (iii), namely ^{256}No [32] and ^{254}Rf [33,34], both subjects of recent K-isomer studies with not yet clearly established characteristics. The first provides the possibility to examine a trio of isomers in No isotopes across the known $N = 152$ deformed subshell closure (see below) while the second provides

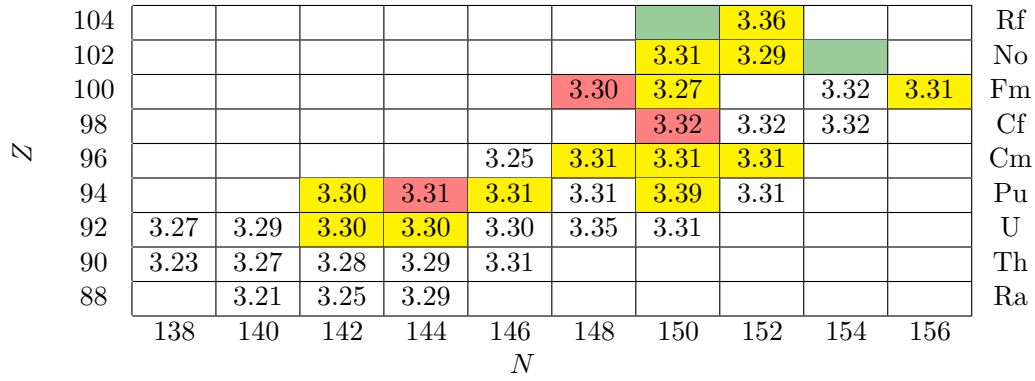

FIG. 1. Ratios $R_{4/2}$ outlining in the (N, Z) plane an area of good-rotor nuclei (with $R_{4/2} \geqslant 3.2$) within the actinide and transfermium region. The color code indicates the criteria under which the nuclei have been selected for this K-isomer study. The color coding is ■ (yellow): nuclei with explicitly documented data on isomeric states [criteria (i) and (ii)]; ■ (red): well-deformed nuclei with isomer-like excitations not explicitly adopted as K isomers [criterion (iii)]; ■ (green): documented isomers in nuclei, assumed to be deformed, but with no data assessing the $R_{4/2}$ value [criterion (iii)].

a continuation of the aforementioned interesting 8^- series in the $N = 150$ isotones.

In Fig. 1 the selected nuclei are visualized in the (N, Z) plane using a color coding corresponding to the criterion under which each isotope has been chosen. Thus, accordingly, calculations have been performed for 18 nuclei: 2 uranium, 4 plutonium, 3 curium, 1 californium, 3 fermium, 3 nobelium, and 2 rutherfordium isotopes.

IV. FIT OF THE PAIRING INTERACTION

Let us discuss now the choice made for the parametrization of the seniority residual interaction to be used in our HF + BCS approach. As discussed in the seminal paper of Bohr, Mottelson, and Pines [35] two quantities deduced from experimental data and accessible to mean-field based calculations, exhibit a clear-cut dependence on pairing correlations: the moments of inertia (MoI) of the first 2^+ states in well-deformed (good rotor) nuclei and the odd-even mass differences (OEMD). In a recent paper [36] it has been shown that upon parametrizing the $|T_z| = 1$ pairing matrix elements G_q, assumed to be constant but charge dependent in the seniority force approximation, as

$$G_q = -\frac{G_0^{(q)}}{11 + N_q}, \quad q = \{n, p\}, \tag{1}$$

where N_q is the total number of particles of charge state q, both MoI and OEMD fitting procedures lead in the rare-earth region to consistent values of the parameters $G_0^{(q)}$ within 1.7% for neutrons and 2.8% for protons in calculations using the Skyrme SIII particle-hole effective interaction [22] as done here. The rms error on the resulting moments of inertia was found, for the sample of 24 even-even nuclei included in the fit, to be equal to 1.75 $\hbar^2\text{MeV}^{-1}$, corresponding roughly to a relative error in the range of 4%. We note in passing that the quality of such a fit assesses the reasonable character of the assumed N_q dependence of the above matrix element parametrization and, at the same time, the quality of the single-particle level densities obtained upon using the SIII interaction.

Taking stock of this result and in view of the slightly easier MoI approach, we have adjusted the above residual interaction parameters $G_0^{(q)}$ with respect to the experimental energies of the 2_1^+ excited states in all selected nuclei of this approach. As shown in Table II, the considered 2_1^+ energies are in general reasonably well reproduced with the following parameter values:

$$G_0^{(n)} = 15.8\,\text{MeV} \quad \text{and} \quad G_0^{(p)} = 0.9\,G_0^{(n)}. \tag{2}$$

Some more important deviation is obtained (for normally deformed solutions) near the well-known $N = 152$ deformed shell closure (see, e.g., [37]). It appears that our calculations exaggerate the neutron gap between the *hole state* $9/2^-$ and the *particle state* $11/2^-$, as well as the bunching of almost

TABLE II. Theoretical (HFBCS) and experimental (where available) energies (in keV) of the first 2_1^+ states of several nuclei in the range $Z = 92$–104. All data are taken from Ref. [25] except for ^{250}Fm taken from [26].

Nucleus	$E_{2_1^+}^{\text{th}}$	$E_{2_1^+}^{\text{exp}}$
^{234}U	42.34	43.50
^{236}U	48.81	45.24
^{236}Pu	40.10	44.63
^{238}Pu	42.93	44.07
^{240}Pu	44.65	42.82
^{244}Pu	46.73	44.20
^{244}Cm	44.13	42.96
^{246}Cm	44.73	42.85
^{248}Cm	41.79	43.40
^{248}Cf	46.97	41.53
^{248}Fm	50.21	46
^{250}Fm	47.70	45
^{256}Fm	61.23	48.12
^{252}No	44.90	46.40
^{254}No	37.40	44.20
^{256}No	49.87	
^{254}Rf	45.69	
^{256}Rf	37.09	44

degenerate *particle states*, leading to an underestimation of the pairing correlations and of the 2_1^+ energy for the ($N = 152$) ^{254}No and ^{256}Rf nuclei and corresponding overestimations for the ($N = 156$) ^{256}Fm nucleus (see Ref. [23] for a discussion of this point).

V. NUMERICAL RESULTS

Before discussing isomeric energies, we first present single-particle spectra of the selected nuclei in their ground states as well as charge radii and nuclear moments in the ground and excited states. This allows us to assess the relevance of the lowest-energy two-quasiparticle configurations, known to be strongly dependent on the effective nuclear interaction and on the equilibrium deformation.

A. Single-particle spectra in ground states

In Fig. 2–6, we show the neutron (left) and proton (right) single-particle energy spectra of all selected nuclei in their $K^\pi = 0^+$ ground states. The degeneracy of each level is thus 2 owing to time-reversal symmetry. In each panel the neutron number N and proton number Z are placed just above the corresponding Fermi level (last occupied sp state). Assuming $J = K$ we can thus deduce the ground-state quantum numbers J^π of neighboring odd-mass nuclei. Within less than a couple of hundreds of keV we find the quantum numbers of the experimental ground state and low-lying rotational bandheads. This is consistent with the good results in an earlier work based on the Bohr-Mottelson unified model [38]. Noticeable disagreements of ground-state spin and parity are found due to

(1) The inversion of the relative position of the neutron $7/2^+$ and $5/2^+$ levels near $N = 148$ (see Fig. 2) according to the experimental ground states of ^{241,243}Pu. This is also hinted at from the ^{239}Pu spectrum in Ref. [38].
(2) the inversion of $5/2^+$ and $5/2^-$ proton levels around $Z = 94$ (see Fig. 3) according to the experimental ground states of odd-mass Am and Np isotopes. According to Ref. [38] these levels come out in the correct order with the SkM* Skyrme parametrization [39] but not with SIII. However, their energy spacing is good with both parameter sets as hinted at from the bandhead spectrum in ^{237}Np (see Fig. 2 of Ref. [38]).
(3) The inversion of $7/2^+$ and $7/2^-$ proton levels around $Z = 100$ (see Fig. 4).

It should be noted that the above inversions do not affect necessarily the corresponding two-quasiparticle isomeric states as their K^π quantum numbers and the associated particle-hole excitation energy could be unaffected.

B. Nuclear charge radii and moments in ground and excited states

In this subsection we briefly present intrinsic bulk quantities, namely charge radii and electric quadrupole moments, and magnetic dipole moments for the isomeric states. The former two (radii and quadrupole moments) are not much affected by the two-quasiparticle excitations that we are investigating, but their study is meant to ensure that the mean-field solutions which we have found do indeed contain the essential physics required for a correct description of the K isomers. On the other hand, as shown below, the magnetic moments serve as a signature of the spin contents of neutron two-quasiparticle configurations in connection with Gallagher's rule [40].

The root-mean square charge radius is calculated from the proton single-particle states $|i\rangle$ as

$$r_c = \sqrt{\left(\sum_i v_i^2 \langle i|\hat{\mathbf{R}}^2|i\rangle + a^2\right)\Big/ Z}\,, \tag{3}$$

where the sum runs over proton states, v_i^2 is the BCS occupation probability of the single-particle state $|i\rangle$, and $\hat{\mathbf{R}}$ is the position operator in the intrinsic frame. The parameter a is the proton radius. We use the rough estimate $a = 0.85$ fm.

The intrinsic charge quadrupole moment is given in terms of the matrix elements of the one-body quadrupole operator $\hat{Q}_{20}$ in the HFBCS solution. This gives

$$Q_c = \sum_i v_i^2 \langle i|\hat{Q}_{20}|i\rangle, \tag{4}$$

where the sum runs again over proton states. Expressions (3) and (4) hold for the ground state as well as for the excited state with blocking.

The calculated charge radii and charge quadrupole moments in the ground state and two-quasiparticle excited states of the selected nuclei are displayed in Table III. Experimental data for these observables in the ground states, as found in Refs. [41,42], are also indicated.

We obtain a good agreement between calculated and experimental charge quadrupole moments, as already noted long ago [43]. A systematic overestimation of r_c is observed, a well known deficiency of the SIII parametrisation (see [22]). Moreover we find virtually no isomeric displacement for the charge radius, whereas a small effect (less than 30 fm^2) is visible in the charge quadrupole moments.

The magnetic dipole moment μ is calculated in the Bohr-Mottelson unified model picture as explained in a previous work [21]. It is the sum of an intrinsic contribution $\mu_{\rm intr}$ and a collective contribution $\mu_{\rm coll}$. The former is defined by

$$\mu_{\rm intr} = \frac{K}{K+1} \sum_{i,q} v_i^2 \left[g_\ell^{(q)} \langle i|\hat{L}_z|i\rangle + g_s^{(q)} \langle i|\hat{S}_z|i\rangle\right], \tag{5}$$

where i runs over all single-particle states of charge q, $\hat{L}_z$ (resp. $\hat{S}_z$) is the projection of the orbital angular momentum (resp. spin) on the quantization axis z, and $g_\ell^{(q)}$ ($g_s^{(q)}$) is the orbital (spin) gyromagnetic factor for the particle of charge q. The collective contribution reads

$$\mu_{\rm coll} = \frac{K}{K+1}\, g_R, \tag{6}$$

where g_R is the collective gyromagnetic ratio of the core. In particular the latter is computed using the Inglis-Belyaev approximation with the single-particle states of positive angular-momentum projection K on the symmetry axis arising

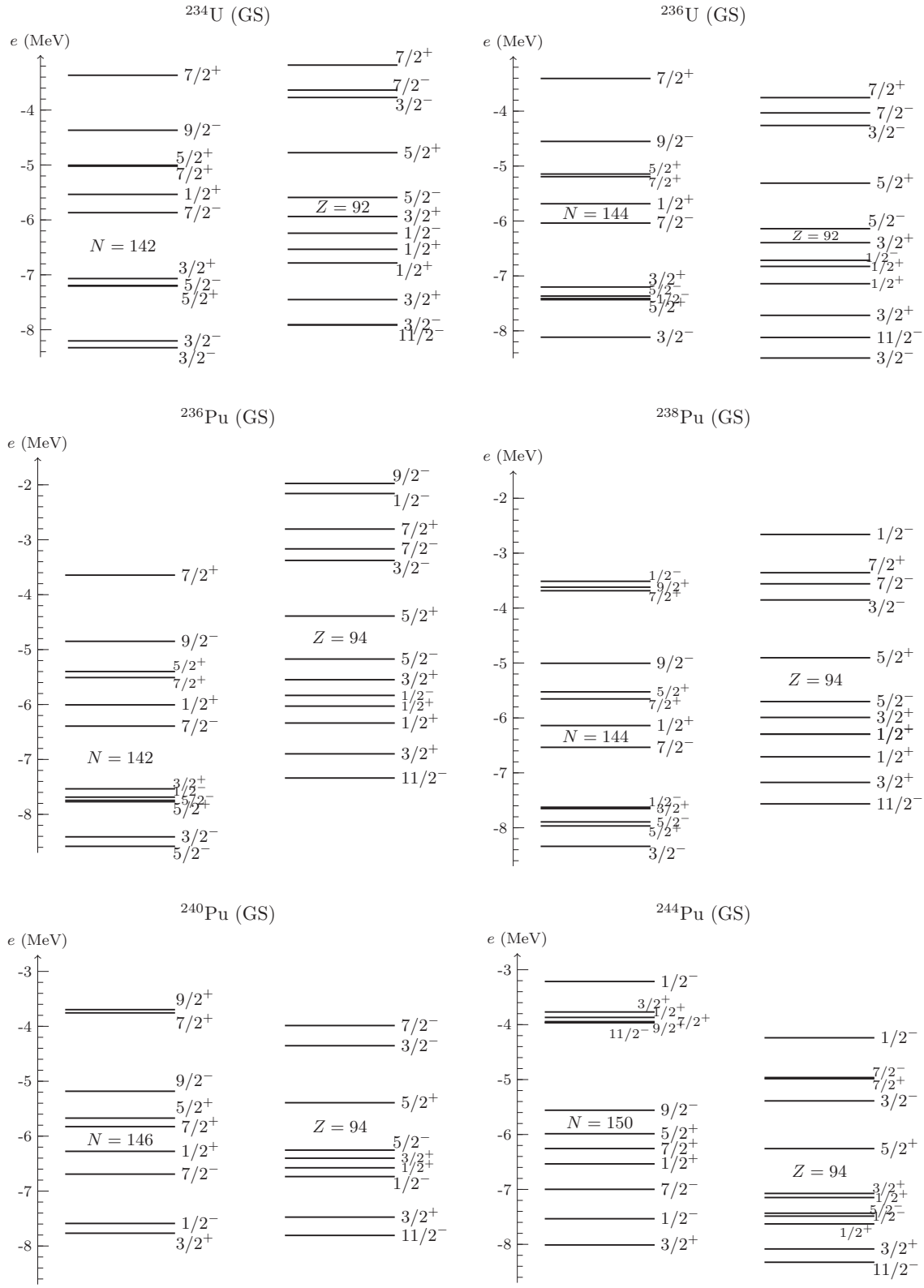

FIG. 2. Single-particle spectra of the considered uranium and plutonium isotopes in their ground state. Neutron and proton energies are respectively displayed on the left and right of each figure.

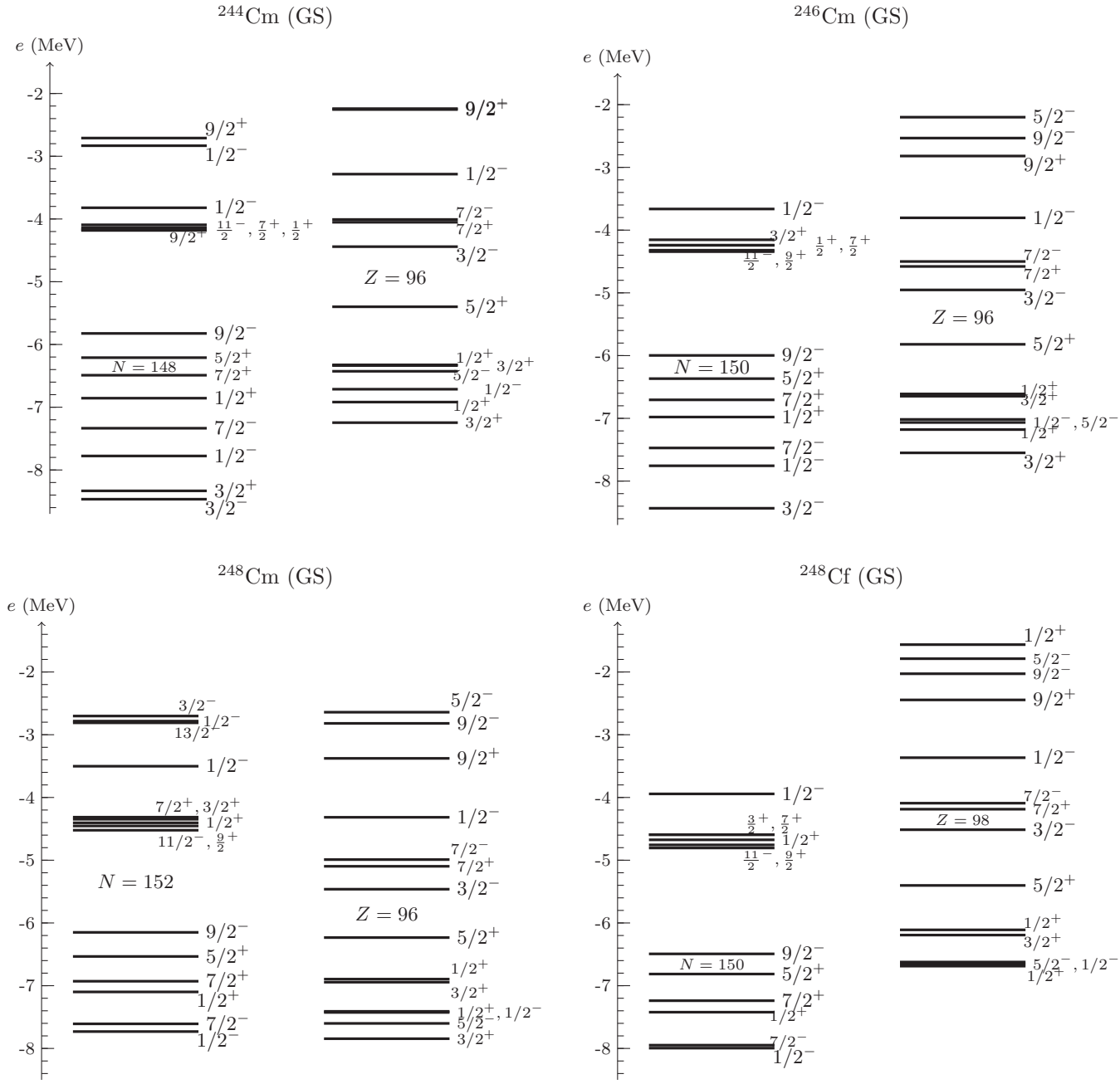

FIG. 3. Same as Fig. 2 for the considered curium and californium isotopes.

from the self-consistent blocked HFBCS solution, excluding the blocked states.

The magnetic moments obtained for the two-quasiparticle excited states in the selected nuclei are given in Table IV. We notice that their values are small and positive (a few tenths of nuclear magneton μ_N) in all considered two-quasineutron configurations except for two cases (^{248}Cm and ^{254}No 8^- isomers). In these configurations, for which $g_\ell^{(n)} = 0$, $\mu_{\rm intr}$ is dominated by the spin contribution of the blocked states $|i_1\rangle$ and $|i_2\rangle$, and one has

$$\mu_{\rm intr} \approx \frac{K}{K+1} g_s^{(n)} (\langle i_1|\hat{S}_z|i_1\rangle + \langle i_2|\hat{S}_z|i_2\rangle). \tag{7}$$

In most of the cases we observe a strong cancellation of the $\langle i_1|\hat{S}_z|i_1\rangle$ and $\langle i_2|\hat{S}_z|i_2\rangle$ matrix elements. It can be ascribed to a dominating antiparallel relative orientation of the intrinsic nucleon spins in the structure of the corresponding sp wave functions which enter the two-quasineutron isomer configurations. This observation may be understood in the context of Gallagher's rule [40]. Indeed, for a given pair of neutron sp states, the lower-lying two-quasiparticle configuration is the one exhibiting antiparallel spin coupling [40], which energetically favors the *K*-isomer formation [44]. In our case this effect yields small negative values of the order of $-0.1\mu_N$ for $\mu_{\rm intr}$. The only two exceptions encountered are in ^{248}Cm and ^{254}No 8^- isomers, both formed over the

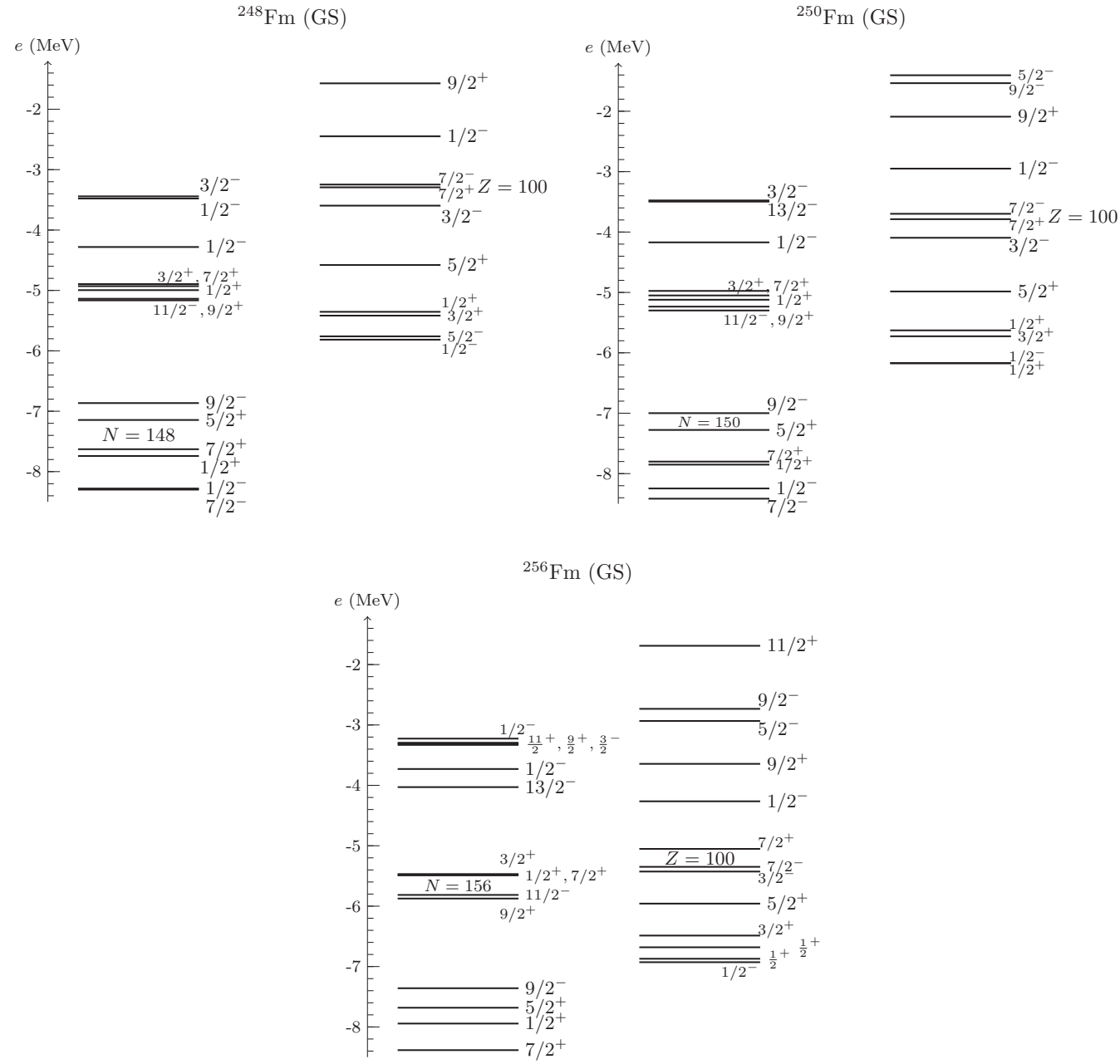

FIG. 4. Same as Fig. 2 for the considered fermium isotopes.

$N = 152$ gap, where we instead find $\langle i_1|\hat{S}_z|i_1\rangle \approx \langle i_2|\hat{S}_z|i_2\rangle \approx 0.4$ (in $\hbar$ units). This gives an indication for the presence of parallel-spin couplings in the corresponding two-quasineutron configurations. On the other hand the collective contribution $\mu_{\rm coll}$ varies only a little over all considered nuclei and configurations, and is of the order of 0.3 to 0.4 (in μ_N units). Hence a small overall value of μ of the order of $0.2\mu_N$ to $0.3\mu_N$ in the two-quasineutron isomeric states is obtained except for the above two cases where one instead finds $\mu \approx -1.7\mu_N$.

In contrast, the magnetic moment of two-quasiproton K isomers is dominated by the orbital contribution of the blocked states with an additive effect in all considered isomers. Because we also find in almost all cases that $\langle i_1|\hat{S}_z|i_1\rangle \approx -\langle i_2|\hat{S}_z|i_2\rangle$, we have $\langle i_1|\hat{L}_z|i_1\rangle + \langle i_2|\hat{L}_z|i_2\rangle \approx K$. Neglecting $\mu_{\rm coll}$ we therefore deduce that the magnetic moment of two-quasiproton K isomers is of the order of $K^2/(K+1)$, as found in Table IV.

We may conclude that the calculated values of the magnetic dipole moment in the considered K-isomeric states carry specific information about the contents of the sp wave functions entering the isomer configurations. Thus, similarly to what is suggested in Ref. [45], we may argue that any future experimental data on magnetic moments would provide a test for

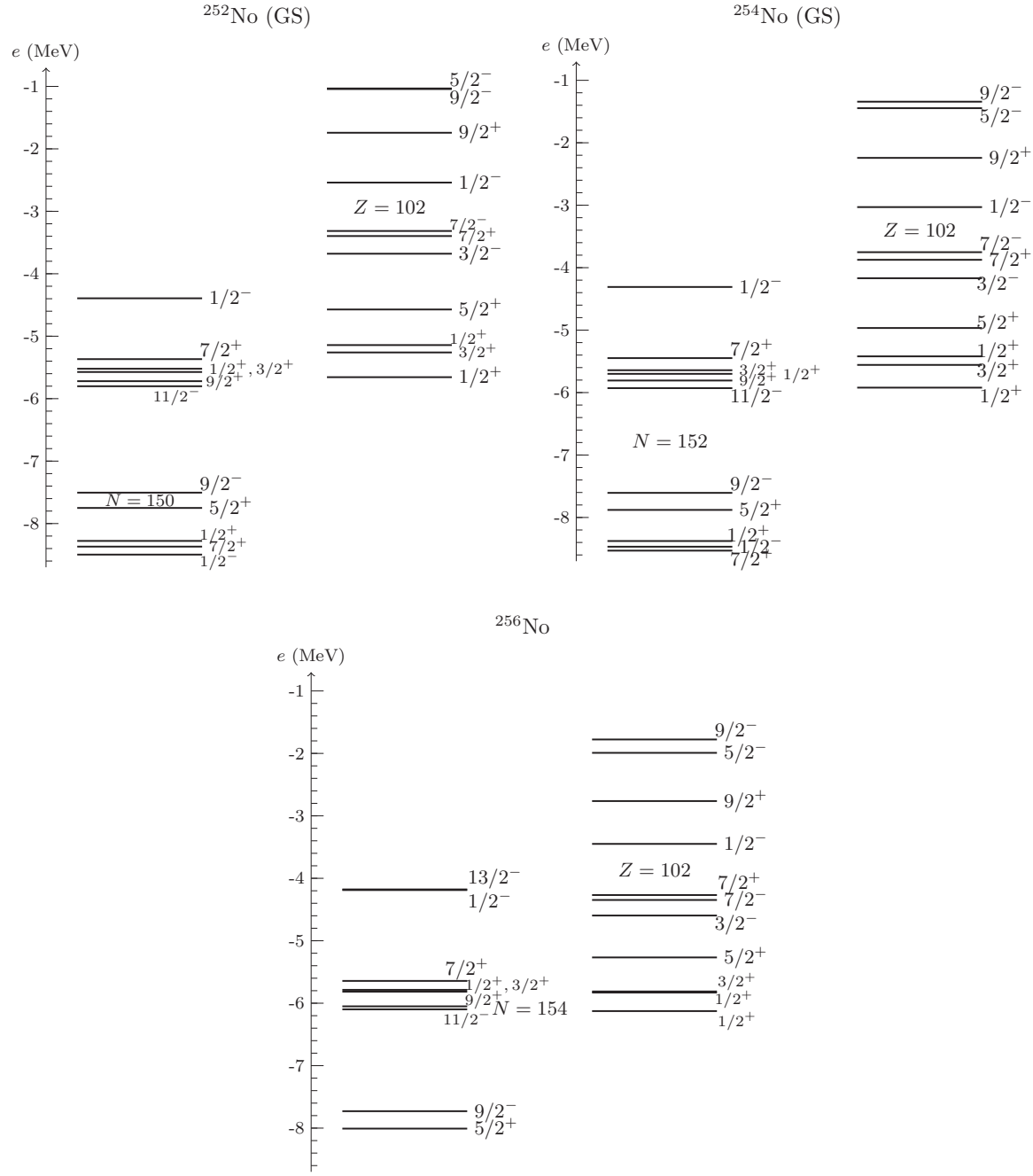

FIG. 5. Same as Fig. 2 for the considered nobelium isotopes.

the relevance of the solutions obtained and the potential applicability of the present approach to resolve the $M1$ (magnetic) decay channel of K isomers.

From the single-particle spectra analysis and the above bulk properties we can gain some confidence in the relevance of our ground- and excited-state solutions.

C. Isomeric energies

Let us now turn to the main topic of the present paper, namely the isomeric energies. Table IV shows their calculated and experimental values for the considered nuclei together with the two-quasiparticle configurations of these excited states.

We start our investigation with the ^{234}U nucleus where we have identified two experimentally well established isomeric states. The 6^- (33.5-μs) isomer is long known as a neutron 2qp configuration $(\frac{7}{2}^-, \frac{5}{2}^+)_n$ [12]. Our calculation overestimates its experimental energy of 1.421 MeV [25,27] by 160 keV. We know for this state that releasing the reflection symmetry in the variation procedure lowers the theoretical value to 1.481 MeV [18] in better agreement with the experiment. However, such a study is beyond the

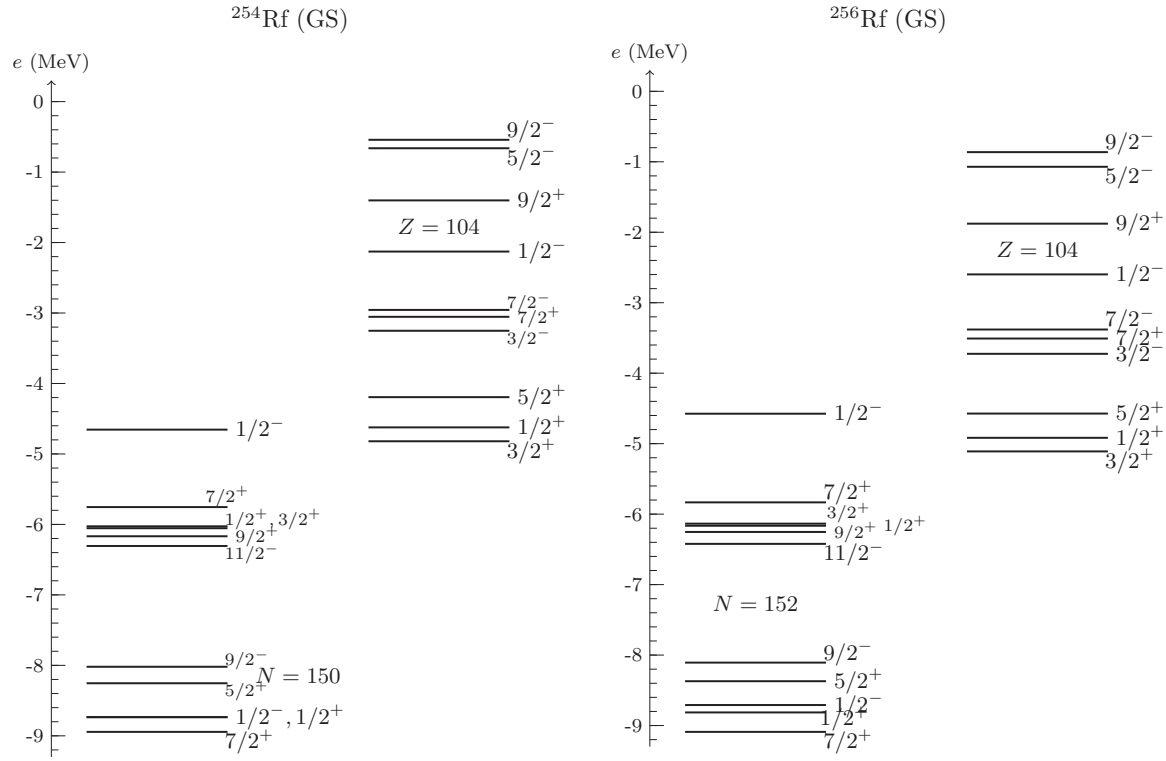

FIG. 6. Same as Fig. 2 for the considered rutherfordium isotopes.

scope of this work since here our aim is to systematically examine the K-isomeric activity in the selected nuclei all on the same footing based on the assumption of reflection symmetry.

The 5^+ state with a half-life of 2.2 ns and an energy of 1.553 MeV [25], recognized as a neutron 2qp configuration $(\frac{5}{2}^+, \frac{5}{2}^+)_n$ [29], is calculated for this configuration to have an excitation energy which overestimates the experimental value by as much as 0.9 MeV. For this state we additionally examined the alternative $(\frac{7}{2}^+, \frac{3}{2}^+)_n$ configuration, which also appears around the neutron Fermi level (see Fig. 2). The corresponding theoretical 5^+ 2qp isomeric energy of 2.348 MeV is slightly closer to the experimental value. These two 5^+ configurations could probably be coupled to provide an energy closer to the data for the lower resulting state. Yet, this should be by far not enough to correct for the observed discrepancy.

From Fig. 2 it is seen that in both configurations the overestimation of the experimental energy is due to the large gap of about 2 MeV between the corresponding orbitals. Since the 6^- isomeric energy is well reproduced, with a blocked neutron configuration $(\frac{5}{2}^+, \frac{7}{2}^-)$, one can conclude that the $\frac{5}{2}^+$ particle state lies too high above the neutron Fermi level.

In ^{236}U the 4^- isomer, assigned to be a neutron $(\frac{7}{2}^-, \frac{1}{2}^+)_n$ configuration [46], is well reproduced by the present calculation, which underestimates the experimental energy by only 25 keV. Also, a rather good theoretical description is obtained for the $5^-(\frac{5}{2}^-, \frac{5}{2}^+)_p$ isomer [47] in ^{236}Pu. The same proton configuration forms a 5^- isomer in ^{240}Pu [49], which is also very well reproduced with a deviation of only 14 keV. We therefore considered worth predicting a $5^-(\frac{5}{2}^-, \frac{5}{2}^+)_p$ state in ^{238}Pu with an isomeric energy of 1.190 MeV. Blocking instead the $-5/2^+$ pairing partner (as defined in Appendix A of Ref. [21]) in the configuration $(\frac{5}{2}^-, -\frac{5}{2}^+)_p$ we describe with a rather good accuracy (with an underestimation of only 23 keV) the excitation energy (1.312 MeV) of a 0^- state in ^{236}Pu. This state could thus be interpreted as a possible 2qp excitation with not yet measured half-life [25].

In ^{238}Pu a 4^-, 8.5-ns isomeric state interpreted as a neutron $(\frac{7}{2}^-, \frac{1}{2}^+)_n$ configuration [29,48] is well reproduced. In ^{240}Pu we have also considered a 3^+ state with a half-life of 1.32 ns interpreted as a neutron $(\frac{5}{2}^+, \frac{1}{2}^+)_n$ 2qp excitation [29]. Our calculation for this configuration provides, however, an energy which overestimates the experiment by more than 300 keV. By looking at the neutron sp spectrum in Fig. 2, we notice that another configuration, $(\frac{7}{2}^+, -\frac{1}{2}^+)_n$, would give a somewhat lower theoretical energy and thus we obtained a slightly better agreement with the experiment.

Of special interest is the isotonic series of 8^- isomers based on the neutron $(\frac{9}{2}^-, \frac{7}{2}^+)_n$ configuration in $N = 150$ isotones. For ^{244}Pu our calculation reproduces remarkably well the experimental isomeric energy within a few keV, but an increasing discrepancy with the experiment is observed

TABLE III. Theoretical and experimental (where available) charge radii r_c and quadrupole moments Q_c in the ground and isomeric states of several nuclei in the range $Z = 92$–104. In the data the italicized numbers refer to the uncertainties in the last digits of the quoted values. The $(8^-)_n$ configuration considered here in ^{254}No is $(\frac{5}{2}^+, \frac{11}{2}^-)_n$.

Nucleus	State	r_c (fm)		Q_c (b)	
		Theory	Expt. [41]	Theory	Expt. [42]
^{234}U	GS	5.902	5.8291 *52*	10.08	10.35 *10*
	$(6^-)_n$	5.901		10.14	
^{236}U	GS	5.916	5.8431 *38*	10.36	10.80 *9*
	$(4^-)_n$	5.917		10.55	
	$(4^-)_p$	5.910		10.14	
^{236}Pu	GS	5.932		10.85	
	$(5^-)_p$	5.936		11.17	
^{238}Pu	GS	5.945	5.8535 *378*	11.10	11.26 *9*
	$(4^-)_n$	5.946		11.21	
	$(5^-)_p$	5.948		11.39	
^{240}Pu	GS	5.958	5.8701 *379*	11.28	11.44 *9*
	$(5^-)_p$	5.960		11.54	
^{244}Pu	GS	5.980	5.8948 *382*	11.35	11.73 *9*
	$(8^-)_n$	5.980		11.50	
^{244}Cm	GS	5.998	5.8429 *181*	12.02	12.14 *8*
	$(6^+)_n$	5.999		12.16	
^{246}Cm	GS	6.008	5.8562 *184*	12.01	12.26 *8*
	$(8^-)_n$	6.008		12.12	
^{248}Cm	GS	6.018	5.8687 *193*	11.99	12.28 *8*
	$(8^-)_n$	6.014		11.72	
^{248}Cf	GS	6.033		12.47	
	$(8^-)_n$	6.033		12.59	
^{248}Fm	GS	6.047		12.78	
	$(6^+)_n$	6.047		12.89	
^{250}Fm	GS	6.057		12.83	
	$(8^-)_n$	6.057		12.94	
^{256}Fm	GS	6.082		12.14	
	$(7^-)_p$	6.083		12.52	
^{252}No	GS	6.081		13.18	
	$(8^-)_n$	6.080		13.26	
^{254}No	GS	6.091		13.18	
	$(8^-)_p$	6.093		13.35	
	$(8^-)_n$	6.090		13.11	
	$(16^+)_{np}$	6.092		13.25	
^{256}No	GS	6.100		12.94	
	$(5^-)_n$	6.101		13.15	
	$(7^-)_n$	6.101		13.15	
^{254}Rf	GS	6.106		13.62	
	$(8^-)_p$	6.104		13.64	
^{256}Rf	GS	6.116		13.64	
	$(5^-)_p$	6.116		13.55	
	$(8^-)_n$	6.120		14.08	

as Z increases, and reaches about 250 keV in ^{252}No. This is not yet well understood. One could remark, however, that in ^{248}Cf, for which the half-life of the 8^- state is not known, our calculation yields a quite good agreement (within 15 keV) with the experiment, which supports its 2qp interpretation. In ^{254}Rf the calculations predict some higher energy of about 1.6 MeV, which may be expected, according to the above trend, to overestimate the future experimental value, which could be measured, e.g., through the methods proposed in Ref. [34].

Apart from the above isotonic series of 8^- isomers in this region, our calculations provide an excellent reproduction of the 34-ms 6^+ isomer in ^{244}Cm with neutron configuration $(\frac{7}{2}^+, \frac{5}{2}^+)_n$ [29,50]. The overestimation of the 148-ms 8^- isomer in ^{248}Cm by about 0.6 MeV may be explained as an effect of the too large $N = 152$ deformed-shell gap.

For the 6^+ isomer in ^{248}Fm we observe, with an overestimation of the isomeric energy of about 50 keV, a rather good agreement with the experiment. A reasonably good description (with an underestimation of about 100 keV) is also obtained for the 7^-, 70-ms isomer in ^{256}Fm with the proton configuration $(\frac{7}{2}^+, \frac{7}{2}^-)_p$ [12,54].

In ^{254}No we interpret the 8^- isomer as a proton $(\frac{7}{2}^-, \frac{9}{2}^+)_p$ configuration [29,56]. Here our calculations overestimate the experimental isomeric energy by about 0.6 MeV. Alternatively, we also considered the neutron configurations $(\frac{5}{2}^+, \frac{11}{2}^-)_n$ and $(\frac{9}{2}^-, \frac{7}{2}^+)_n$ for which, however, the overestimation already approaches and exceeds 1 MeV. This result may be explained by the specific structure (overestimated shell gap) of the neutron sp spectrum around the deformed magic number $N = 152$ obtained in our HFBCS calculation. At the same time it is interesting to note that the proton-neutron combinations of the above configurations may form a four-quasiparticle (4qp) configuration which could correspond to the 184-μs 16^+ isomer in ^{254}No as claimed in Ref. [6]. Although our calculations strongly overestimate the experimental energy assigned to this isomeric activity, the mechanism of 4qp configuration formation clearly resembles the one of the 16^+, 31-yr isomer of ^{178}Hf [57] and, therefore, calls for a further detailed study.

Extending our analysis to ^{256}No, we have considered the isomeric activity observed at an energy known merely by its lower bound of 1.089 MeV (with a half-life of 7.8 μs in Ref. [32]). We confirm the relevance of the assignment (5^- or 7^-) made in this publication as being obtained by the coupling of a $11/2^-$ neutron sp state with either a $-1/2^+$ or a $3/2^+$ neutron sp state by calculating such states at about 0.4 MeV above the quoted lower bound.

Finally, completing the set of selected nuclei and isomers, we performed calculations for the tentative 5^- and 8^- isomers in ^{256}Rf with, respectively, the proton and neutron configurations $(\frac{1}{2}^-, \frac{9}{2}^+)_p$ and $(\frac{7}{2}^-, \frac{9}{2}^+)_n$ [58]. Given the large uncertainties in the experimental energies of both states [25,27], one can only assert that the theoretical predictions are found to be in a reasonable proximity of the tentative experimental energy values. Recent lifetimes measurements in ^{256}Rf suggest a rather rich and puzzling K-isomer activity [59] calling for further detailed experimental and theoretical work in this nucleus.

Summarizing the above results, one can say that an overall good model description of isomeric energies is obtained. An appropriate quasiparticle-structure interpretation can be given for the considered K-isomeric states and for the states which are potential candidates for K isomerism. More pre-

TABLE IV. Theoretical (HFBCS) magnetic moments and excitation energies obtained for K^π isomeric states with given 2qp configurations for several nuclei in the range $Z = 92$–104. The associated experimental isomeric energies and half-lives are also given. The qp structure of the isomers resulting from our calculations is displayed, being in most cases in agreement with previous assignments, whose references are given. References to relevant experimental work are also listed in the last column. In addition, for reasons explained in the text, we add a proton 2qp 5^- state in ^{238}Pu, a neutron 2qp 8^- state in ^{254}No, and the 4qp 16^+ isomeric state in ^{254}No.

Nucl.	N	K^π	2qp config., Refs.	μ (μ_N)	$E^*_{\rm HFBCS}$ (MeV)	$E^*_{\rm exp}$ (MeV)	$T^{\rm exp}_{1/2}$	Experiment Refs.
^{234}U	142	6^-	$(\frac{7}{2}^-, \frac{5}{2}^+)_n$ [12]	+0.23	1.582	1.421	33.5 (20) μs	[25,27]
		5^+	$(\frac{5}{2}^+, \frac{5}{2}^+)_n$ [29]	−0.02	2.425	1.553	2.20 (25) ns	[25,29]
			$(\frac{7}{2}^+, \frac{3}{2}^+)_n$	+0.18	2.348			
^{236}U	144	4^-	$(\frac{7}{2}^-, \frac{1}{2}^+)_n$ [46]	+0.17	1.028	1.053	100 (4) ns	[25,27]
^{236}Pu	142	5^-	$(\frac{5}{2}^-, \frac{5}{2}^+)_p$ [47]	+4.23	1.138	1.186	1.2 (3) μs	[25,27]
		0^-	$(\frac{5}{2}^-, -\frac{5}{2}^+)_p$	0	1.289	1.312		[25]
^{238}Pu	144	5^-	$(\frac{5}{2}^-, \frac{5}{2}^+)_p$	+4.24	1.190			
		4^-	$(\frac{7}{2}^-, \frac{1}{2}^+)_n$ [29,48]	+0.23	1.033	1.083	8.5 (5) ns	[25]
^{240}Pu	146	3^+	$(\frac{5}{2}^+, \frac{1}{2}^+)_n$ [29]	−0.04	1.367	1.031	1.32 (15) ns	[25]
			$(\frac{7}{2}^+, -\frac{1}{2}^+)_n$	+0.30	1.245			
		5^-	$(\frac{5}{2}^-, \frac{5}{2}^+)_p$ [49]	+4.24	1.295	1.309	165 (10) ns	[25,27]
^{244}Pu	150	8^-	$(\frac{9}{2}^-, \frac{7}{2}^+)_n$ [28]	+0.28	1.219	1.216	1.75 (12) s	[25,28]
^{244}Cm	148	6^+	$(\frac{7}{2}^+, \frac{5}{2}^+)_n$ [29,50]	+0.12	1.042	1.040	34 (2) ms	[25,27]
^{246}Cm	150	8^-	$(\frac{9}{2}^-, \frac{7}{2}^+)_n$ [51,52]	+0.32	1.227	1.180	1.12 (24) s	[25,51,52]
^{248}Cm	152	8^-	$(\frac{9}{2}^-, \frac{7}{2}^+)_n$ [52]	−1.72	2.025	1.461	146 (18) μs	[52]
^{248}Cf	150	8^-	$(\frac{9}{2}^-, \frac{7}{2}^+)_n$ [30,51]	+0.31	1.276	1.261		[25]
^{248}Fm	148	6^+	$(\frac{5}{2}^+, \frac{7}{2}^+)_n$ [31]	+0.09	1.240	1.188	10.1 (6) ms	[31,53]
^{250}Fm	150	8^-	$(\frac{9}{2}^-, \frac{7}{2}^+)_n$ [26]	+0.32	1.374	1.199	1.92 (5) s	[26,27]
^{256}Fm	156	7^-	$(\frac{7}{2}^+, \frac{7}{2}^-)_p$ [12,54]	+6.31	1.312	1.426	70 (5) ms	[25,27]
^{252}No	150	8^-	$(\frac{9}{2}^-, \frac{7}{2}^+)_n$ [51,55]	+0.36	1.501	1.253	109 (3) ms	[25,27]
^{254}No	152	8^-	$(\frac{7}{2}^-, \frac{9}{2}^+)_p$ [29,56]	+7.31	1.914	1.297	263 (2) ms	[25,27]
			$(\frac{5}{2}^+, \frac{11}{2}^-)_n$	−1.65	2.209			
			$(\frac{9}{2}^-, \frac{7}{2}^+)_n$	−1.70	2.327			
		16^+	$(\frac{9}{2}^-, \frac{7}{2}^+)_n(\frac{7}{2}^-, \frac{9}{2}^+)_p$	+5.66	4.142	2.930	184 (2) μs	[25,27]
			$(\frac{5}{2}^+, \frac{11}{2}^-)_n(\frac{7}{2}^-, \frac{9}{2}^+)_p$	+5.71	3.892			
^{256}No	154	(5^-)	$(\frac{11}{2}^-, -\frac{1}{2}^+)_n$ [32]	+0.23	1.487	>1.089	$7.8^{+8.3}_{-2.6}$ μs	[32]
		(7^-)	$(\frac{11}{2}^-, \frac{3}{2}^+)_n$ [32]	+0.23	1.448			
^{254}Rf	150	(8^-)	$(\frac{9}{2}^-, \frac{7}{2}^+)_p$ [33]	+0.36	1.647		4.7(1) μs	[25,33,34]
^{256}Rf	152	(5^-)	$(\frac{1}{2}^-, \frac{9}{2}^+)_p$ [58]	+4.49	1.028	≈1.120	25(2) μs	[25,27]
		(8^-)	$(\frac{7}{2}^-, \frac{9}{2}^+)_p$ [58]	+7.33	1.748	≈1.400	17(2) μs	

cisely, a good agreement for isomeric energies is found with a root-mean-square deviation of about 0.37 MeV. The largest discrepancies are about 0.9 MeV for the 5^+ state in ^{234}U and about 1 MeV for the 8^- and 16^+ states in ^{254}No, which we believe are due to the too large energy gap in the neutron sp spectrum around the $N = 152$ deformed shell closure. If we discard these three states, we obtain a root-mean-square deviation of only 0.15 MeV.

VI. SUMMARY AND CONCLUSIONS

We have implemented a comprehensive study of the K-isomeric states in heavy well-deformed actinide and heavier nuclei. To this end we applied the Skyrme HF + BCS energy-density functional with axial and parity symmetries, and with self-consistent blocking for the isomeric states. Special attention has been devoted to the adjustment of pairing matrix elements in this mass region, to best reproduce the excitation energy of the 2^+_1 state assuming a good-rotor spectrum. For the 18 retained nuclei we have calculated the ground-state energies and identified relevant 2qp configurations describing K isomers. From the corresponding blocked solutions we have calculated the isomeric energies and compared them with experimental data. With the exception of a few cases (see below), we have obtained a rms deviation of about 150 keV. These exceptions are found in ^{234}U and ^{254}No. They can

be ascribed to single-particle properties of the Skyrme SIII parametrization. More precisely, this is the $\frac{5}{2}^+$ particle state which lies too high above the $N = 142$ neutron Fermi level in ^{234}U. One obtains an overestimated shell gap around the $N = 152$ deformed magic number in ^{254}No and, in addition, a too large bunching of particle states.

Bearing in mind the overall good quality of the obtained isomeric energies in the actinide region and some transfermium nuclei, we expect that the present SEDF approach possesses some predictive capability in identifying relevant two-quasiparticle configurations and assessing their excitation energies beyond the considered mass region (larger A and/or Z numbers). This perspective entails the need of some further improvements and extensions.

One direction in this respect is to try avoiding the BCS low pairing-correlation regimes encountered in the 2qp states. This can be achieved by applying in a fully self-consistent way the so-called highly truncated diagonalizaton approach (HTDA), allowing one to describe such correlations in a restricted space of particle-hole excitations [9].

Another direction is to study the relevance of reflection-asymmetric solutions. This would allow us to take into account the possible presence of octupole deformed shapes as hinted at from the work of Ref. [18]. The possible existence of a softness of the potential energy surface, as a function of a relevant intrinsic parity breaking mode parameter, could also play a role in defining the isomeric wave function. A possible way to look at such quantal shape fluctuations may be, for instance, as suggested in Ref. [60]. Study along these two directions is a subject of forthcoming works.

ACKNOWLEDGMENTS

This work has been done in the framework of and supported by the PHC Rila 2019 France-Bulgaria agreement under Contract No. 43184NJ and contract No. KP-06-RILA/6 with the Bulgarian National Science Fund (BNSF). We also gratefully acknowledge interesting discussions with O. Dorveau and B. Gall.

[1] P. Ring and P. Schuck, *The Nuclear Many-Body Problem* (Springer-Verlag, New York, 1980).
[2] P. M. Walker and G. D. Dracoulis, Nature (London) **399**, 35 (1999).
[3] G. D. Dracoulis, P. M. Walker, and F. G. Kondev, Rep. Prog. Phys. **79**, 076301 (2016).
[4] R.-D. Herzberg and P. T. Greenlees, Prog. Part. Nucl. Phys. **61**, 674 (2008).
[5] F.-Q. Chen *et al.*, J. Phys. G: Nucl. Part. Phys. **40**, 015101 (2013).
[6] R.-D. Herzberg *et al.*, Nature (London) **442**, 896 (2006).
[7] V. G. Soloviev, Kgl. Dan. Vid. Selsk. Mat. Fys. Skr. **1**(11), 1 (1961).
[8] S. G. Nilsson and O. Prior, Mat. Fys. Medd. Dan. Vid. Selsk. **32**(16), 1 (1961).
[9] N. Pillet, P. Quentin, and J. Libert, Nucl. Phys. A **697**, 141 (2002).
[10] M. J. A. de Voigt, J. Dudek, and Z. Szymański, Rev. Mod. Phys. **55**, 949 (1983).
[11] G. G. Andersson, S. E. Larsson, G. Leander, P. Möller, S. G. Nilsson, I. Ragnarsson, S. Åberg, R. Bengtsson, J. Dudek, B. Nerlo-Pomorska, K. Pomorski, and Z. Szymański, Nucl. Phys. A **268**, 205 (1976).
[12] V. G. Soloviev and T. Siklos, Nucl. Phys. **59**, 145 (1964).
[13] S. K. Tandel, T. L. Khoo, D. Seweryniak, G. Mukherjee, I. Ahmad, B. Back, R. Blinstrup, M. P. Carpenter, J. Chapman, P. Chowdhury, C. N. Davids, A. A. Hecht, A. Heinz, P. Ikin, R. V. F. Janssens, F. G. Kondev, T. Lauritsen, C. J. Lister, E. F. Moore, D. Peterson, P. Reiter, U. S. Tandel, X. Wang, and S. Zhu, Phys. Rev. Lett. **97**, 082502 (2006).
[14] H. L. Liu, F. R. Xu, P. M. Walker, and C. A. Bertulani, Phys. Rev. C **83**, 011303(R) (2011).
[15] P. Walker and N. Minkov, Phys. Lett. B **694**, 119 (2010).
[16] N. Minkov and P. Walker, Phys. Scr. **89**, 054021 (2014).
[17] G. G. Adamian, N. V. Antonenko, and W. Scheid, Phys. Rev. C **81**, 024320 (2010).
[18] L. Bonneau, P. Quentin, N. Minkov, D. Ivanova, J. Bartel, H. Molique, and M.-H. Koh, Bulg. J. Phys. **46**, 366 (2019).
[19] J.-P. Delaroche, M. Girod, H. Goutte, and J. Libert, Nucl. Phys. A **771**, 103 (2006).
[20] K. E. Karakatsanis, G. A. Lalazissis, V. Prassa, and P. Ring, Phys. Rev. C **102**, 034311 (2020).
[21] L. Bonneau, N. Minkov, D. D. Duc, P. Quentin, and J. Bartel, Phys. Rev. C **91**, 054307 (2015).
[22] M. Beiner, H. Flocard, N. Van Giai, and P. Quentin, Nucl. Phys. A **238**, 29 (1975).
[23] P. Quentin, L. Bonneau, N. Minkov, D. Ivanova, J. Bartel, H. Molique, and M.-H. Koh, Bulg. J. Phys. **48**, 634 (2021).
[24] H. Flocard, P. Quentin, A. K. Kerman, and D. Vautherin, Nucl. Phys. A **203**, 433 (1973).
[25] http://www.nndc.bnl.gov/ensdf/.
[26] P. T. Greenlees, R. D. Herzberg, S. Ketelhut, P. A. Butler, P. Chowdhury, T. Grahn, C. Gray-Jones, G. D. Jones, P. Jones, R. Julin, S. Juutinen, T. L. Khoo, M. Leino, S. Moon, M. Nyman, J. Pakarinen, P. Rahkila, D. Rostron, J. Saren, C. Scholey, J. Sorri, S. K. Tandel, J. Uusitalo, and M. Venhart, Phys. Rev. C **78**, 021303(R) (2008).
[27] A. K. Jain, B. Maheshwari, S. Garg, M. Patial, and B. Singh, Nucl. Data Sheets **128**, 1 (2015).
[28] S. S. Hota, S. K. Tandel, P. Chowdhury, I. Ahmad, M. P. Carpenter, C. J. Chiara, J. P. Greene, C. R. Hoffman, E. G. Jackson, R. V. F. Janssens, B. P. Kay, T. L. Khoo, F. G. Kondev, S. Lakshmi, S. Lalkovski, T. Lauritsen, C. J. Lister, E. A. McCutchan, K. Moran, D. Peterson, U. Shirwadkar, D. Seweryniak, I. Stefanescu, Y. Toh, and S. Zhu, Phys. Rev. C **94**, 021303(R) (2016).
[29] F. P. Heßberger *et al.*, Eur. Phys. J. A **43**, 55 (2010).
[30] K. Katori, I. Ahmad, and A. M. Friedman, Phys. Rev. C **78**, 014301 (2008).
[31] F. G. Kondev, G. D. Dracoulis, and T. Kibedi, At. Data Nucl. Data Tables **103–104**, 50 (2015).
[32] K. Kessaci, B. J. P. Gall, O. Dorvaux, A. Lopez-Martens, R. Chakma, K. Hauschild, M. L. Chelnokov, V. I. Chepigin, M.

Forge, A. V. Isaev, I. N. Izosimov, D. E. Katrasev, A. A. Kuznetsova, O. N. Malyshev, R. Mukhin, J. Piot, A. G. Popeko, Y. A. Popov, E. A. Sokol, A. I. Svirikhin, M. S. Tezekbayev, and A. V. Yeremin, Phys. Rev. C **104**, 044609 (2021).

[33] H. M. David, J. Chen, D. Seweryniak, F. G. Kondev, J. M. Gates, K. E. Gregorich, I. Ahmad, M. Albers, M. Alcorta, B. B. Back, B. Baartman, P. F. Bertone, L. A. Bernstein, C. M. Campbell, M. P. Carpenter, C. J. Chiara, R. M. Clark, M. Cromaz, D. T. Doherty *et al.*, Phys. Rev. Lett. **115**, 132502 (2015).

[34] J. Khuyagbaatar *et al.*, Nucl. Phys. A **994**, 121662 (2020).

[35] Å. Bohr, B. R. Mottelson, and D. Pines, Phys. Rev. **110**, 936 (1958).

[36] N. M. Nor, N.-A. Rezle, K.-W. Kelvin-Lee, M.-H. Koh, L. Bonneau, and P. Quentin, Phys. Rev. C **99**, 064306 (2019).

[37] I. Ahmad, R. R. Chasman, and P. R. Fields, Phys. Rev. C **61**, 044301 (2000).

[38] M. H. Koh, D. D. Duc, T. V. Nhan Hao, H. T. Long, P. Quentin, and L. Bonneau, Eur. Phys. J. A **52**, 3 (2016).

[39] J. Bartel, P. Quentin, M. Brack, C. Guet, and H.-B. Håkansson, Nucl. Phys. A **386**, 79 (1982).

[40] C. J. Gallagher, Jr., Phys. Rev. **126**, 1525 (1962).

[41] I. Angeli and K. P. Marinova, At. Data Nucl. Data Tables **99**, 69 (2013).

[42] S. Raman, C. W. Nestor, Jr. and P. Tikkanen, At. Data Nucl. Data Tables **78**, 1 (2001).

[43] H. Flocard, P. Quentin, and D. Vautherin, Phys. Lett. B **46**, 304 (1973).

[44] P. M. Walker and F. R. Xu, Phys. Scr. **91**, 013010 (2016).

[45] N. Minkov and P. M. Walker, Eur. Phys. J. A **48**, 80 (2012).

[46] H. F. Brinckmann *et al.*, Phys. Lett. B **43**, 386 (1973).

[47] M. Asai *et al.*, Eur. Phys. J. A **23**, 395 (2005).

[48] B. Bengtson, J. Jensen, M. Moszynki, and H. L. Nielsen, Nucl. Phys. A **159**, 249 (1970).

[49] A. H. Wapstra and P. F. A. Goudsmit, Physica **37**, 273 (1967).

[50] Y. A. Lazarev *et al.*, Phys. Scr. **39**, 422 (1989).

[51] A. P. Robinson *et al.*, Phys. Rev. C **78**, 034308 (2008).

[52] U. Shirwadkar, S. K. Tandel, P. Chowdhury, T. L. Khoo, I. Ahmad, M. P. Carpenter, J. P. Greene, R. V. F. Janssens, F. G. Kondev, T. Lauritsen, C. J. Lister, D. Peterson, D. Seweryniak, X. Wang, and S. Zhu, Phys. Rev. C **100**, 034309 (2019).

[53] S. Ketelhut, Rotational Structures and High-K Isomerism in ^{248,250}Fm, PhD. thesis, University of Jyvaskyla, 2010 (unpublished).

[54] H. L. Hall, K. E. Gregorich, R. A. Henderson, D. M. Lee, D. C. Hoffman, M. E. Bunker, M. M. Fowler, P. Lysaght, J. W. Starner, and J. B. Wilhelmy, Phys. Rev. C **39**, 1866 (1989).

[55] B. Sulignano, C. Theisen, J. P. Delaroche, M. Girod, J. Ljungvall, D. Ackermann, S. Antalic, O. Dorvaux, A. Drouart, B. Gall, A. Gorgen, P. T. Greenlees, K. Hauschild, R. D. Herzberg, F. P. Hessberger, U. Jakobsson, P. Jones, R. Julin, S. Juutinen, S. Ketelhut, W. Korten *et al.*, Phys. Rev. C **86**, 044318 (2012).

[56] R. M. Clark *et al.*, Phys. Lett. B **690**, 19 (2010).

[57] Y. Sun *et al.* Phys. Lett. B **589**, 83 (2004).

[58] J. Rissanen, R. M. Clark, K. E. Gregorich, J. M. Gates, C. M. Campbell, H. L. Crawford, M. Cromaz, N. E. Esker, P. Fallon, U. Forsberg, O. Gothe, I. Y. Lee, H. L. Liu, A. O. Machiavelli, P. Mudder, H. Nitsche, G. Pang, A. Rice, D. Rudolph, M. A. Stoyer, A. Wiens, and F. R. Xu, Phys. Rev. C **88**, 044313 (2013).

[59] J. Khuyagbaatar, H. Brand, R. A. Cantemir, C. E. Dullmann, M. Gotz, S. Gotz, F. P. Hessberger, E. Jager, B. Kindler, J. Krier, N. Kurz, B. Lommel, B. Schausten, and A. Yakushev, Phys. Rev. C **103**, 064303 (2021).

[60] F. Q. Chen, Y. X. Liu, Y. Sun, P. M. Walker, and G. D. Dracoulis, Phys. Rev. C **85**, 024324 (2012).